Supplementary Figures

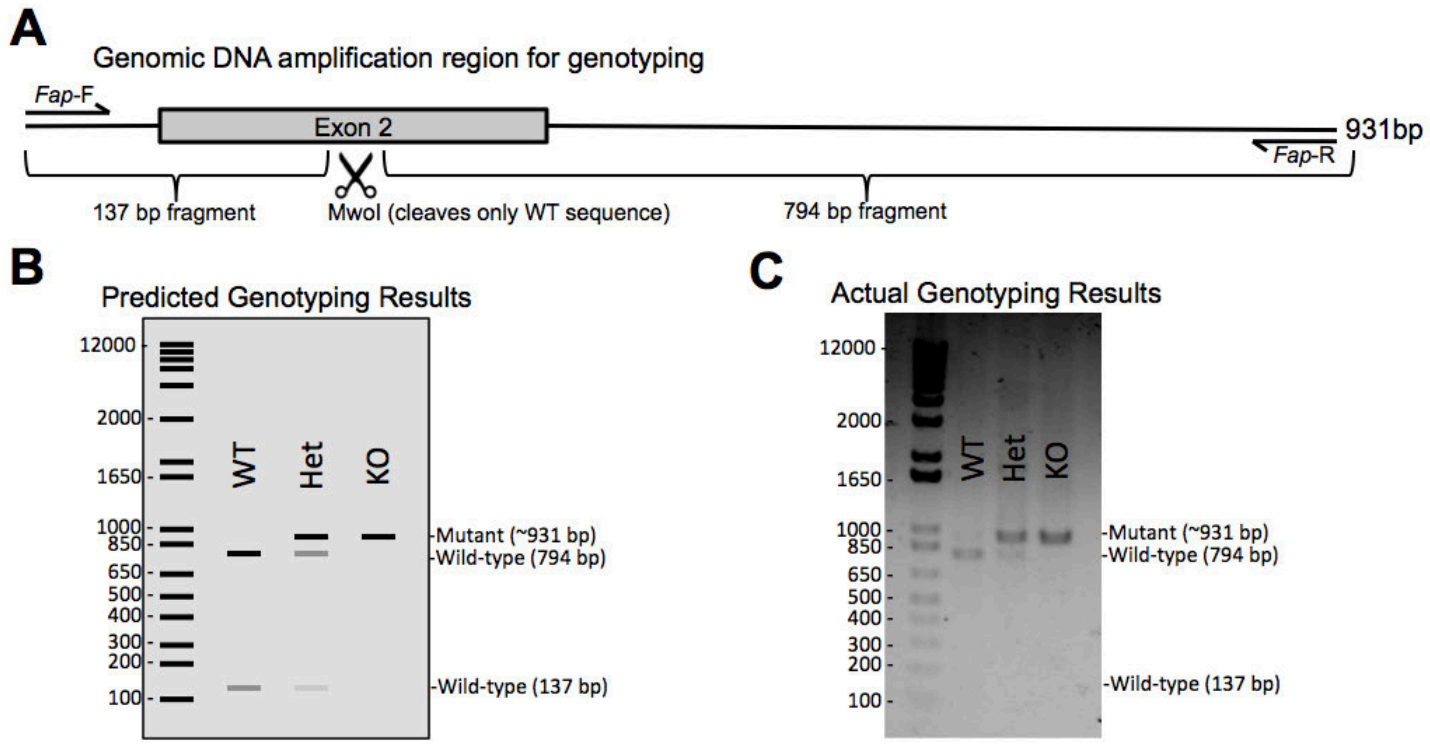

Figure S1: Genotyping of *Fap*$^{-/-}$ mouse lines using restriction enzyme digestion. Genotyping primers were designed to flank Exon 2, including targeted CRISPR/Cas9 mutagenesis site, to amplify a 931bp segment of genomic DNA. After PCR amplification, the product is subjected to digestion by Mwo1, which results in near complete digestion of wild-type (WT) PCR product. Partial digestion occurs for heterozygous (Het) samples, and no digestion occurs for knockout (KO) samples. **A)** Primer map of genomic DNA fragment, including Exon 2, Mwo1 cleavage site, and predicted fragment sizes. **B)** Predicted genotyping results and band sizes. **C)** Actual genotyping results for all genotypes.

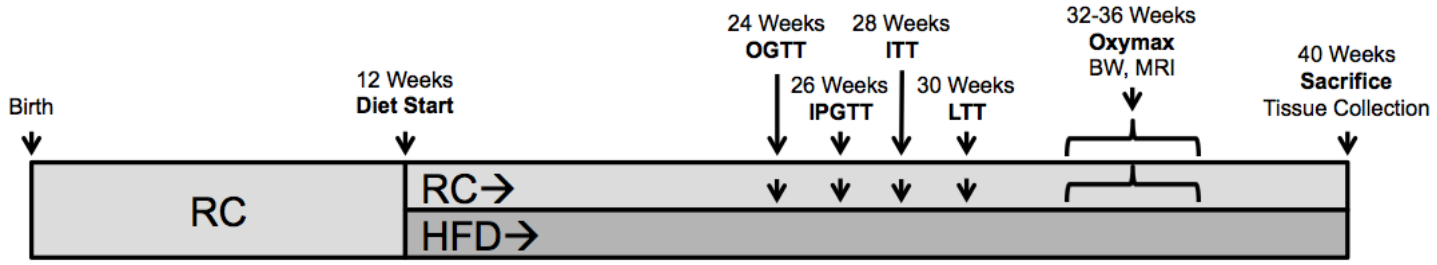

Figure S2: Chronic RC and HFD experimental timeline. All mice are raised on rodent chow (RC) and then at 12 weeks of age are assigned to continue on RC or be switched to 45% high-fat diet (HFD). Beginning at 24 weeks, mice are subjected to oral glucose tolerance test (OGTT), intraperitoneal glucose tolerance test (IPGTT), insulin tolerance test (ITT), lipid tolerance test (LTT) in 2 week intervals. Between 32-36 weeks of age, the mice have body-composition measurements, and are then placed in individual Oxymax chambers in random order for indirect calorimetry and food intake measurements. At 40 weeks of age, the mice are sacrificed and tissues collected for protein and mRNA analyses. In HFD-fed mice, body-weights (BW) are measured periodically, including on test days, to monitor weight gain over time.

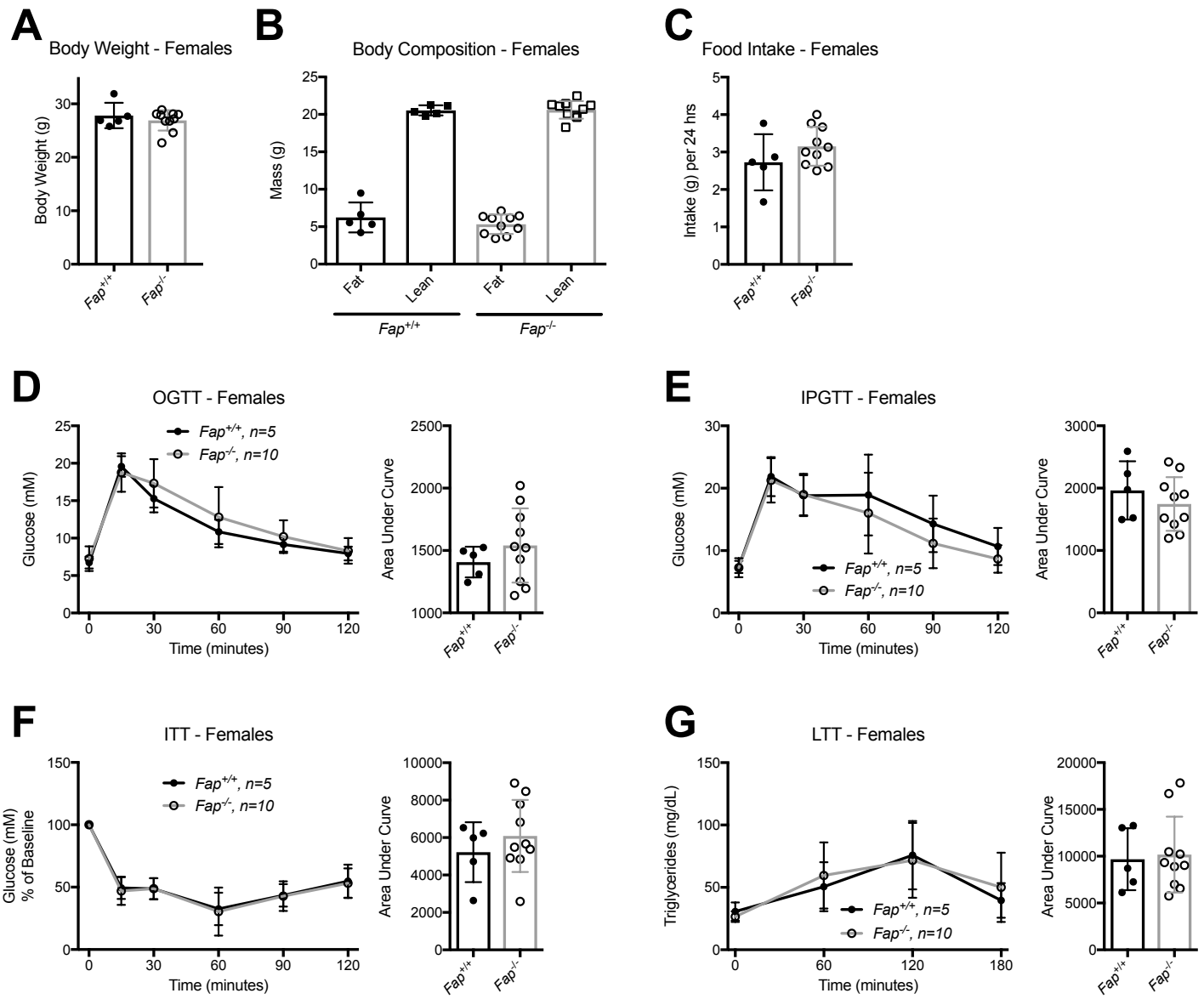

Figure S3: Female *Fap*$^{-/-}$ mice fed normal rodent chow exhibit normal glucose and lipid tolerance. Female mice were subjected to the same treatment as RC-fed male mice (Figure S3) and studied simultaneously. **A)** Body weight. **B)** Body composition. **C)** Food intake. **D)** OGTT and AUC analysis. **E)** IPGTT and AUC analysis. **F)** ITT and AUC analysis. **G)** TGs during LTT and AUC analysis. AUC data was further analyzed using two-tailed *t*-test.

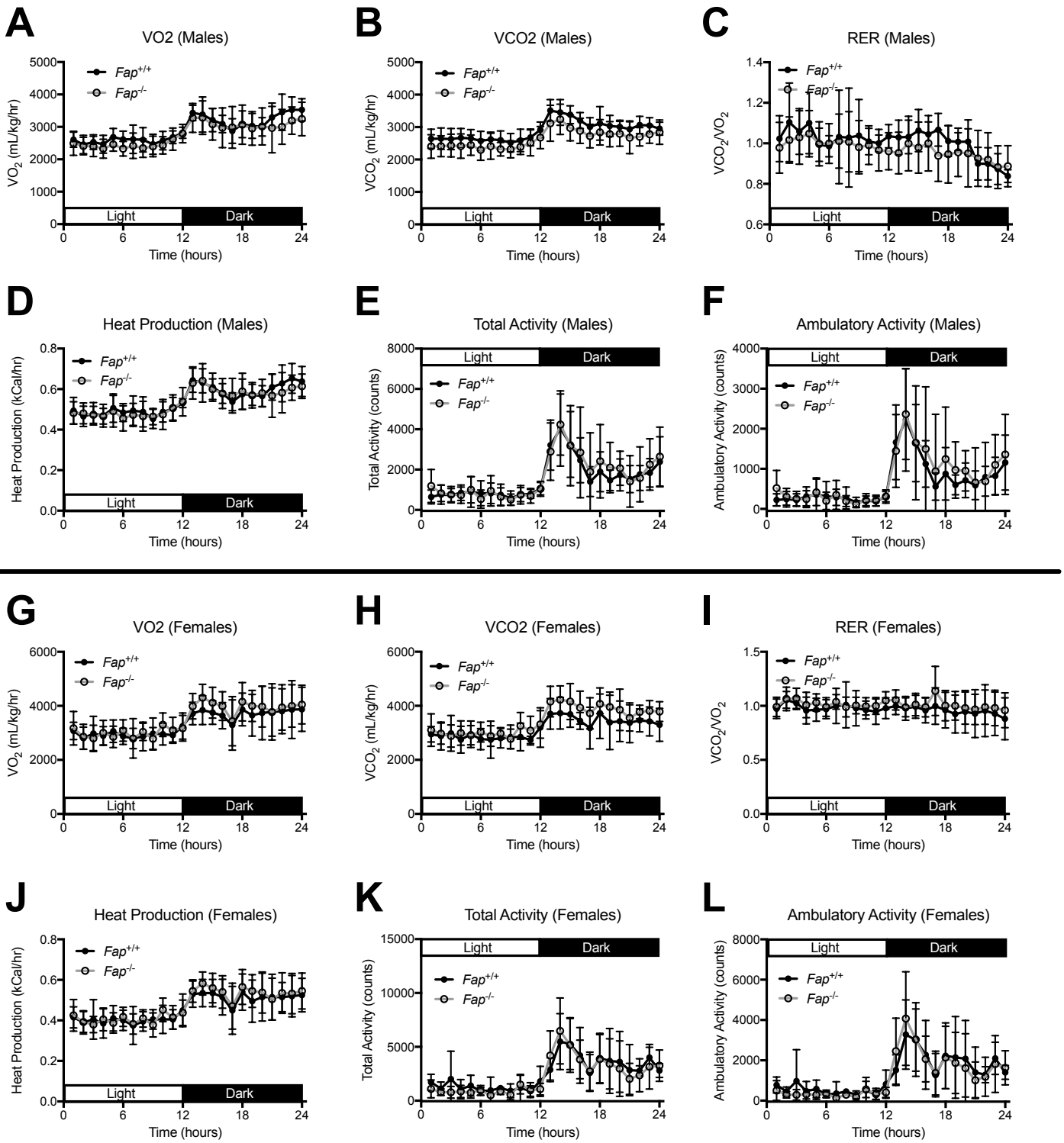

Figure S4: Parameters of energy expenditure are similar in *Fap*$^{-/-}$ vs. *Fap*$^{+/+}$ mice on a RC diet. Adult male and female Fap+/+ and -/- mice underwent indirect calorimetry measurement of several metabolic parameters. **A-F)** Measurements of VO_2, VCO_2, RER, Heat Production, Total Activity, and Ambulatory Activity in male mice. **G-L)** Corresponding measurements of VO_2, VCO_2, RER, Heat Production, Total Activity, and Ambulatory Activity in female mice. Because there were no differences in body weight or body composition, all expenditure values are normalized to body weight.

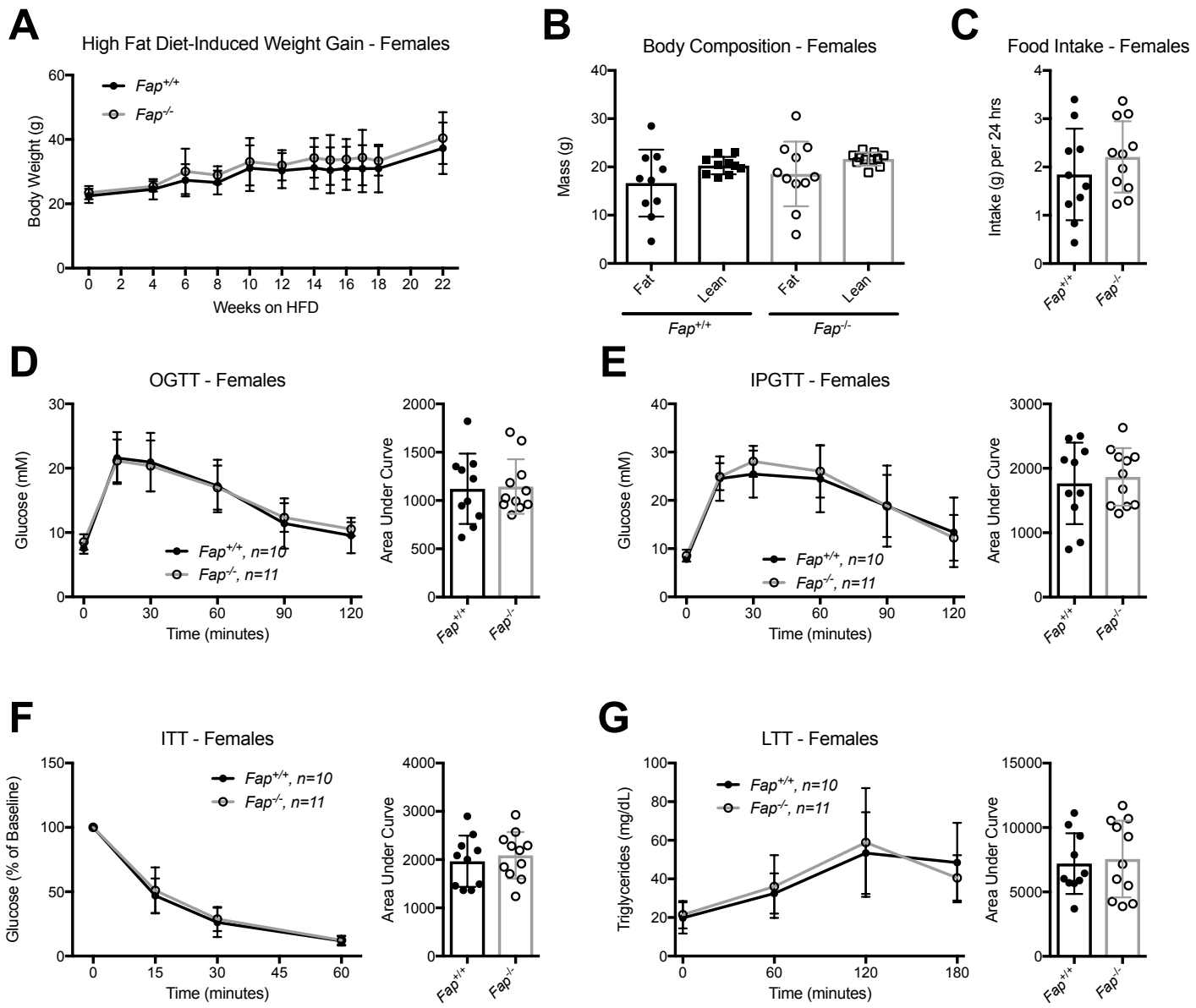

Figure S5: Female *Fap*$^{-/-}$ mice fed chronic high-fat diet exhibit no metabolic defects. Female mice were subjected to the same treatment as the RC-fed male mice Figure S3) and studied simultaneously. **A)** Body weight. **B)** Body composition. **C)** Food intake. **D)** OGTT and AUC analysis. **E)** IPGTT and AUC analysis. **F)** ITT and AUC analysis. **G)** TGs during LTT and AUC analysis. AUC data was analyzed using two-tailed *t*-test.

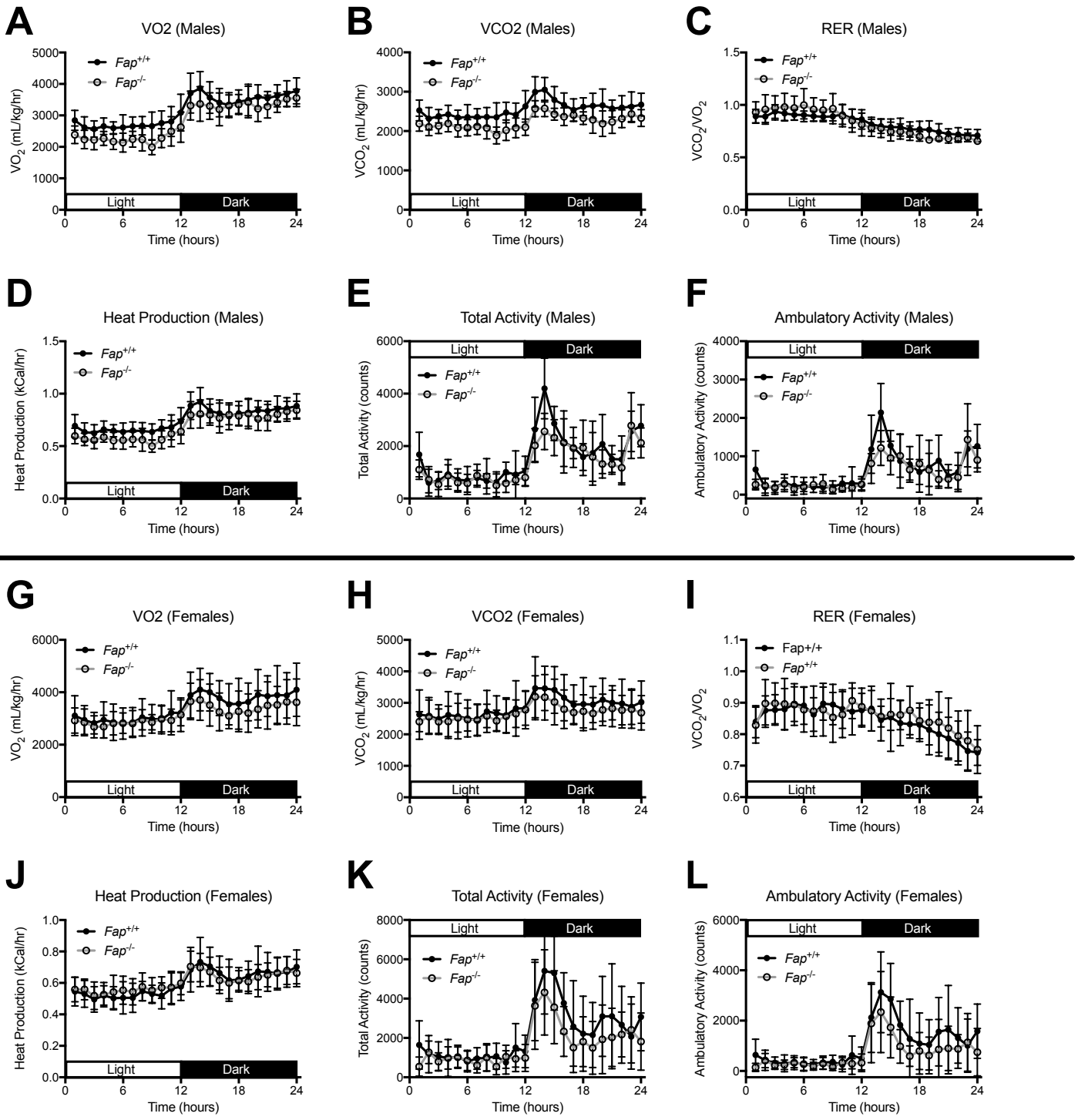

Figure S6: *Fap*$^{-/-}$ mice are metabolically similar to *Fap*$^{+/+}$ mice when fed a normal RC diet. Adult male and female *Fap*$^{+/+}$ and $^{-/-}$ mice underwent indirect calorimetric measurement of several metabolic parameters. **A-F)** Measurements of VO_2, VCO_2, RER, Heat Production, Total Activity, and Ambulatory Activity in male mice. **G-L)** Corresponding measurements of VO_2, VCO_2, RER, Heat Production, Total Activity, and Ambulatory Activity in female mice. Because there were no differences in body weight or body composition, all expenditure values are normalized to body weight.

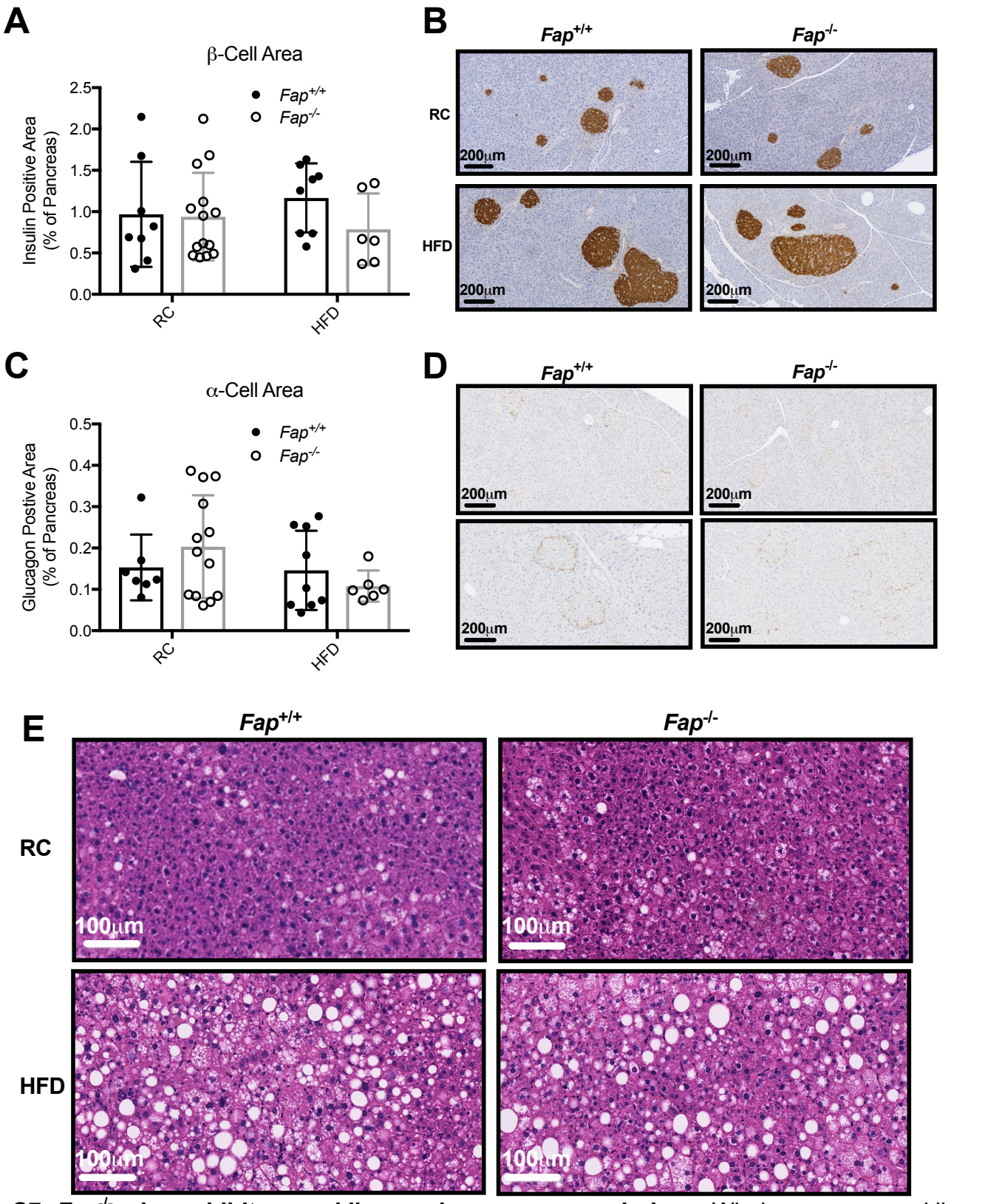

Figure S7: *Fap*$^{-/-}$ mice exhibit normal liver and pancreas morphology. Whole pancreas and liver was removed from 40-week old male *Fap*$^{+/+}$ and *Fap*$^{-/-}$ fed either chronic RC of HFD. Sections mounted on slides for either insulin or glucagon (pancreas) or H&E stained (liver). **A)** β-Cell area (insulin-positive area) or **B)** Representative insulin-stained sections from each experimental condition. **C)** α-Cell area (glucagon-positive area). **D)** Representative glucagon-stained sections from each condition. **E)** Representative H&E-stained liver images from each experimental condition. No statistical significance was detected using 2-way ANOVA.

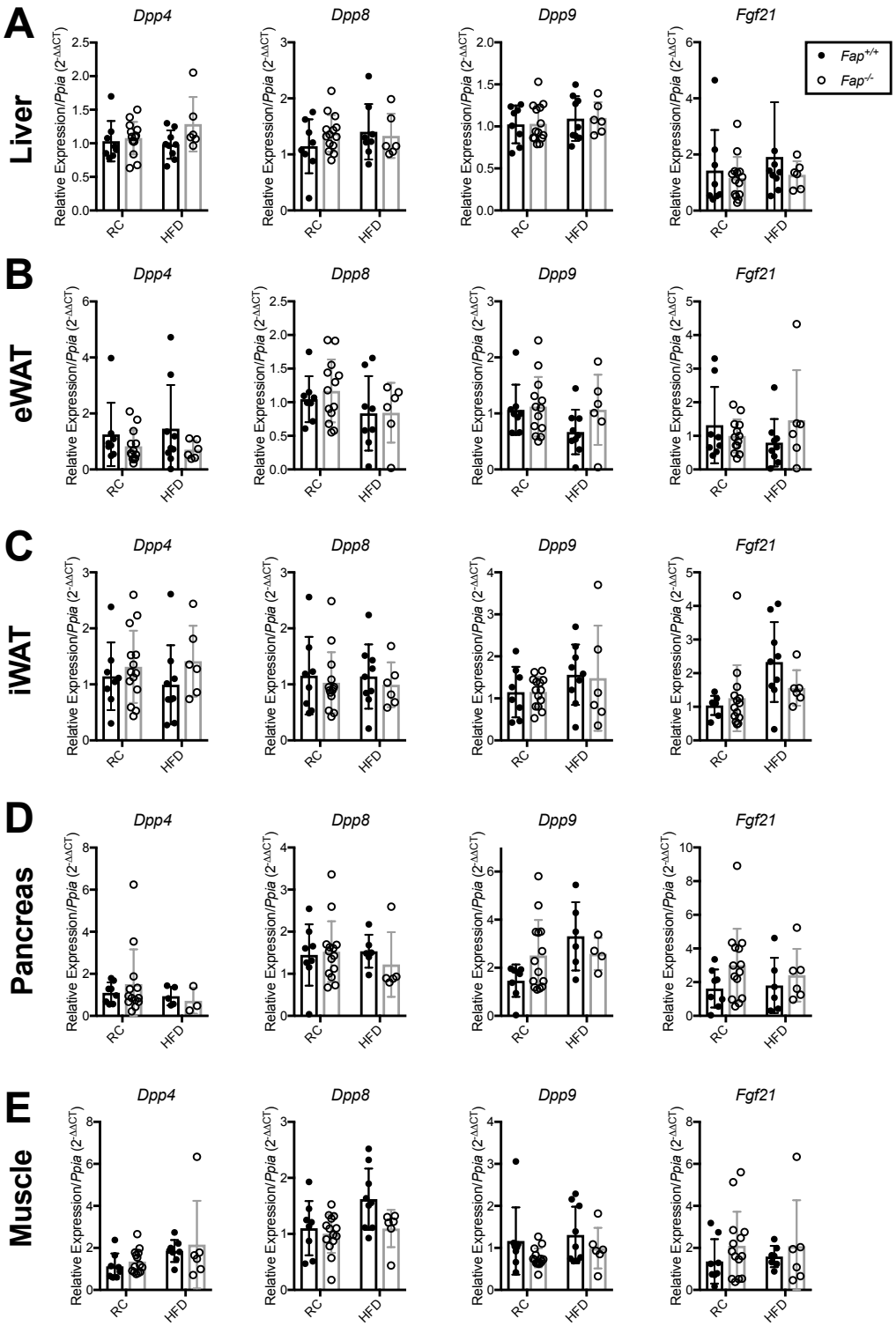

Figure S8: ***Gene expression analysis of DASH family and*** **Fgf21** ***mRNA transcripts*** Tissues were collected from 40-week old male *Fap*$^{+/+}$ and *Fap*$^{-/-}$ mice following chronic RC or HFD feeding. Expression levels of *Dpp4*, *Dpp8*, *Dpp9*, and *Fgf21* mRNA were measured in the listed tissues and expressed relative to levels of endogenous control mRNA, *Ppia,* and normalized to *Fap*$^{+/+}$ RC animals ($2^{-\Delta\Delta CT}$). **A)** Liver. **B)** Epididymal white adipose tissue (eWAT). **C)** Inguinal white adipose tissue (iWAT). **D)** Pancreas. **E)** Muscle. All data were analyzed using 2-way ANOVA and no significant differences were found.

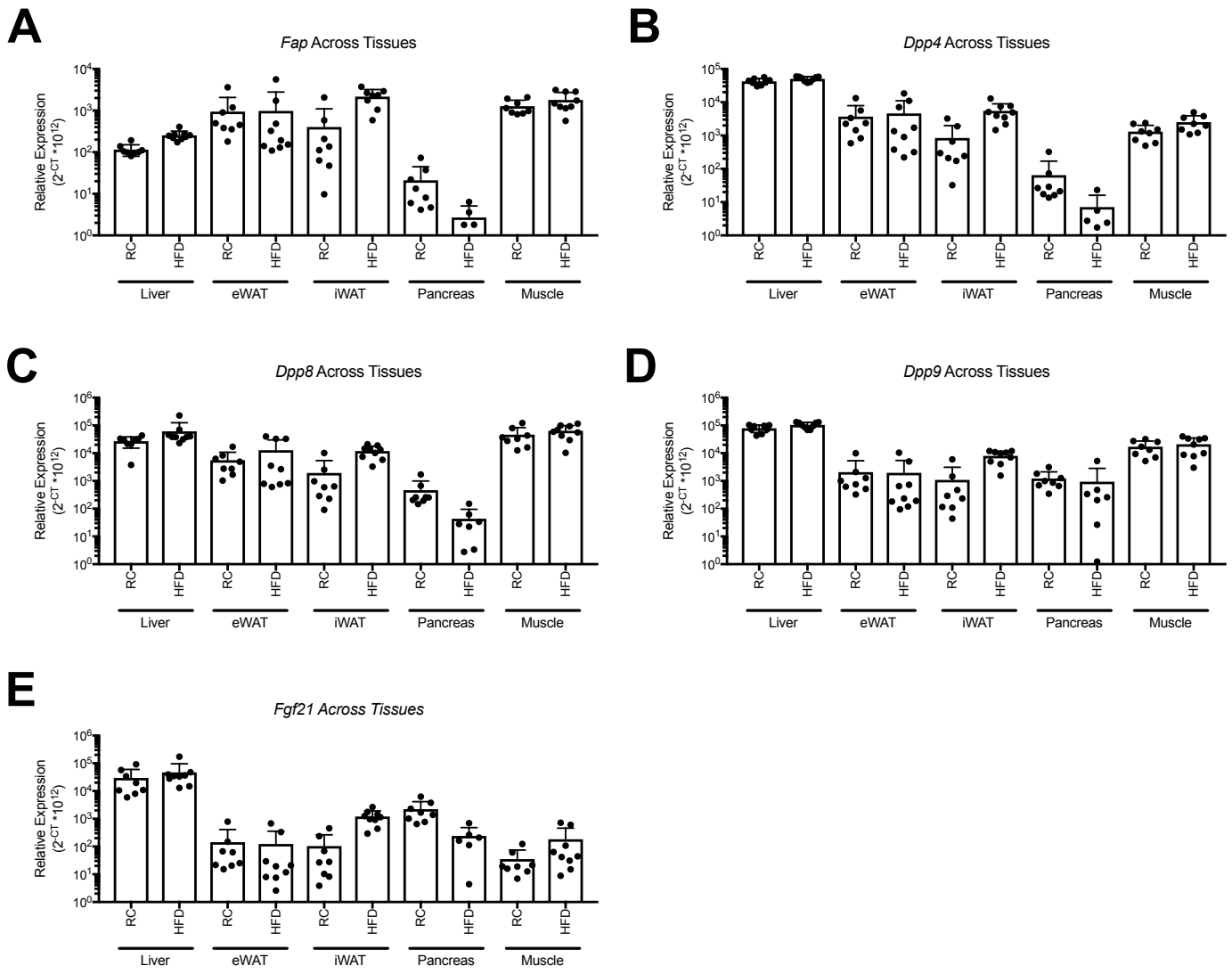

Figure S9: Relative tissue expression profiles of *Fap*, *Dpp4*, *Dpp8*, *Dpp9*, and *Fgf21*. Tissues were collected from 40-week old male $Fap^{+/+}$ mice following chronic RC or HFD feeding. Expression levels of *Fap*, *Dpp4*, *Dpp8*, *Dpp9*, and *Fgf21* mRNA were measured in the listed tissues and expressed as $2^{-CT}X10^{12}$ to estimate relative expression levels of each gene across liver, epididymal white adipose tissue (eWAT), inguinal white adipose tissue (iWAT), pancreas, and muscle. **A)** *Fap* expression across tissues. **B)** *Dpp4* expression across tissues. **C)** *Dpp8* expression across tissues. **D)** *Dpp9* expression across tissues. **E)** *Fgf21* expression across tissues.